Manipulating Etch Selectivities in XeF_2 Vapour Etching

Markus Rondé, Anthony J. Walton, Jonathan G. Terry

***Abstract*— The vapour etching of silicon sacrificial layers is often a critical process in the fabrication of micro/nanosystems. This method has a number of attractive features, in particular, high etch rates of sacrificial silicon layers and good selectivities associated with photoresist, SiO_2, stoichiometric Si_3N_4 and a number of regularly used metal films. However, materials that are commonly inert to XeF_2 are etched when located in the proximity of a silicon sacrificial layer. This proximity is a common situation in the fabrication of such systems and can become a critical issue affecting process control and device reliability. This work uses test structures that have been designed to be very sensitive, thereby delivering much lower selectivities then are typically reported in the literature. This sensitive quantification of the proximity effect is used to evaluate methods designed to improve the selectivity. This work suggests that a reduction in the processing temperature from 25°C to 10°C increases the Si: PECVD SiN selectivity by 68%. However, a more easily implemented modification is to flow hydrogen into the reaction chamber. This method improves the Si: PECVD SiN selectivity by an order of magnitude and the Si: LPCVD SiN selectivity between 200% and 600%.**

***Index Terms*—Vapour Etching, XeF_2, Selectivity, Proximity effect**

I. Introduction

The etching of sacrificial silicon with XeF_2 vapour in order to release free-standing structures in micro- and nanosystems has a number of benefits. High undercut etch rates of up to 40 μm/min have been achieved [1]. Stiction [2] [3] does not occur during processing, and high selectivities towards photoresist, silicon dioxide (SiO_2), stoichiometric, low pressure chemical vapour deposited silicon nitride (LPCVD Si_3N_4), silicon carbide (SiC), aluminum and plasma enhance chemical vapour deposited silicon nitride (PECVD Si:N:H) have been reported [4] [5] [6] [7] [8]. However, there is a growing body of evidence that some of these selectivities are significantly reduced if these layers are positioned in the proximity of the sacrificial silicon layer [9] [10] [11] (referred to as the 'proximity effect'). This issue can complicate the fabrication and design process of MEMS significantly, inhibiting the development of devices and reducing yields and process reliability. The following work investigates the impact of the proximity effect on the etch rates of a range of commonly used materials, and investigates methods than can be applied to improve their selectivity.

Veyan et al. [9] were the first to observe the rapid proximity etching of SiO_2. The authors of this current work reported silicon to PECVD silicon nitride selectivities as low as 5:4 [10]. Research conducted by Hefty et al. [12]–[14], suggests that a fluorine radical of the XeF_2 molecule is removed at a dangling bond of the silicon surface. The remaining XeF molecule remains in the gas phase. It can either lose the remaining fluorine on another dangling bond or disintegrate forming both a xenon and a fluorine radical. This highly reactive fluorine radical might collide with either the silicon or a material in its vicinity. During sacrificial etching, the probability of collision with the other material increases, because the reactive fluorine radicals are trapped underneath the structural layer. The conclusion is that any material that can be etched by fluorine radicals is prone to attack when in proximity to the silicon sacrificial layer. This hypothesis is evaluated in this work by proximity etching a number of materials commonly used in MEMS devices, which are known to be etched by fluorine. PECVD SiO_2, LPCVD Si_3N_4 and PECVD SiN (Si:N:H) were selected because the fluorine etch mechanisms involved have been extensively researched in the context of plasma etching.

To investigate improvements in the etch selectivity, four general mechanisms known to change etch selectivities have been identified from the broader literature:

1) The Arrhenius equations suggest that adjusting the temperature may have a greater effect on the reaction rate of one material than that of another [15] [16] [17] [18]. In the case of XeF_2 etching of Si, it has been observed that the etch rate dependence on temperature follows a "U-curve". The highest reaction rate occurs at 150 K, below which the XeF_2 condenses on the surface. The rate gradually decreases to 20% of the maximum etch rate as the temperatures rise from 150 to 400 K. Beyond this low point at 400 K, the reaction

Manuscript received October 12, 2020; revised November 30, 2020; accepted December 05, 2020. Date of publication xx.xx.xxxx; date of current version xx.xx.xxxx.

Markus Rondé's work was supported by the EPSRC CDT in Sensing and Measurement EP/L016753/1 and the CENSIS Studentship Award programme.

The authors are with the Institute of Integrated Micro and Nano Systems a part of the School of Engineering of the University of Edinburg located at EH9 3FF Edinburgh, UK (e-mail:. markus.ronde@ed.ac.uk).

Color versions of one or more of the figures in this article are available online at https://ieeexplore.ieee.org. Digital Object Identifier xxx .

rate increases again with rising temperature. The experiment was conducted at a pressure of 10^{-8} Torr [19].
2) In some cases, the addition of gases can passivate the surface of otherwise reactive materials, making them inert to the etchant [20] [21].

3) In other cases, the addition of gases can alter the products of the etch. For example, hydrogen additions have been reported to significantly improve the selectivity of fluorine-based etch processes [22], [23].

(4) Sugano et al. [24] observed that the selectivity of Si: Si_3N_4 and Si: SiO_2 decreases from 488:1 to 29:1 and from 5287:1 to 281:1 respectively if the samples are exposed to 3 Wcm^{-2} of UV light at a wavelength of 310 – 340 nm. Another study by Streller et al. [25] suggested that XeF_2 dissociates into XeF and F if excited by ultraviolet light with short wavelength (<150 nm).

This paper focuses on the first and the third of these four mechanisms, the adjustment of the processing temperature and the addition of gases. Firstly, the equipment, test structures and measurement method used during this experiment are detailed, after which the results from the XeF_2 vapour etching proximity effect characterization are presented and discussed. Various samples with SiO_2, LPCVD Si_3N_4 and PECVD SiN structural (target) layers were etched at pressures of 3 – 9 Torr, XeF_2 gas flows of 15 – 35 sccm and temperatures 5°C - 45°C. The impact on the selectivities, when adding hydrogen to the gas mix, is also presented.

II. EQUIPMENT, TEST STRUCTURE AND METHOD

A commercial memsstar Alpha Orbis XeF_2 etch tool was used in this work. In contrast to most of the previously published research on XeF_2 etching, the memsstar tool continuously supplies $XeF_2$to the reaction chamber (rather than in pulses), In addition the processing pressures are comparatively high (up to 10 Torr). The chamber temperature is controllable and can be adjusted to values between 3°C and 45 °C in increments of 0.1°C. Nitrogen is used as a carrier gas to transport the XeF_2 into the reaction chamber, and additional gases can be added to the mix.

A customized test structure and measurement method were developed for this experiment. A detailed description of the design, fabrication procedure and measurement method, as well as a thorough characterization, have been previously presented [10]. The test structures were designed to measure the selectivity between a target layer and a sacrificial layer. It should be stressed that the selectivities measured are specific to the layout and architecture of the test structures, which have been specifically designed to ensure very close proximity of the materials being evaluated. As a result, the selectivity values measured using the test structures may be significantly poorer than those quoted elsewhere.

The test structure consists of an array of aluminum bridges that are suspended above the sacrificial layer, which in turn sits above the target layer. In these experiments, the target layer was

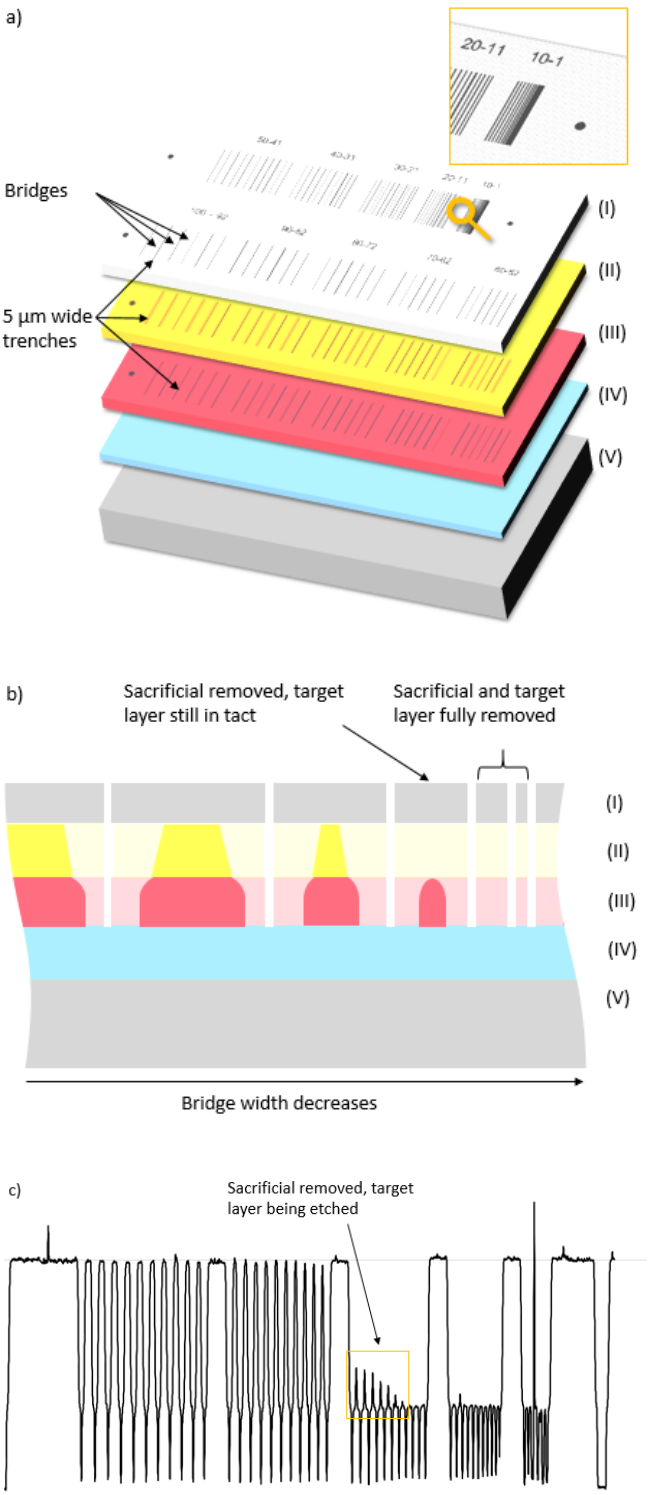

Fig. 1 Graphic depiction of the functionality of the test structure. Showing the layout in a) and a cross-section of a partially etched structure in b); where (I) is the capping, (II) the sacrificial, (III) the target, and (IV) the etch stop layer; (V) represents the substrate. c) Shows an example surface profiler from an etched array.

TABLE I

LAYER CONFIGURATION OF THE SAMPLES USED

Layer Description	**SiN-Reference**	**SiN-PECVD**	**SiN-LPCVD**	**SiO_2-Reference**	**SiO_2-PECVD**
Capping Layer	350 nm Aluminium	350 nm Aluminium	350 nm Aluminium	350 nm Aluminium	350 nm Aluminium
Sacrificial Layer	-	500 nm Polysilicon	500 nm Polysilicon	-	500 nm Polysilicon
Target Layer	450 nm PECVD SiN	450 nm PECVD SiN	500 nm LPCVD Si_3N_4	500 nm PECVD SiO_2	500 nm PECVD SiO_2
Etch Stop	50 nm Platnium	50 nm Platnium	500 nm SiO_2	50 nm Platnium	50 nm Platnium
Adhesion Layer	10 nm Ti	10 nm Ti	-	10 nm Ti	10 nm Ti
Wafer	Silicon	Silicon	Silicon	Silicon	Silicon

either silicon nitride or silicon dioxide. In this case, the width of the bridges increases in increments of 1 µm in the width range between 2 µm and 50 µm and in increments of 2 µm for the 50 µm to 100 µm wide bridges. These values are sufficient to measure etch selectivties at a range from 1.5:1 to 50: 1 with an undercut resolution of 500 nm.. All bridges are 300 µm long. In a previous study, the selectivities were found to be independent of the bridge length. The 300 µm long bridges are a trade-off between the requirement to minimize the real estate required by the test structure on a production wafer and the requirement to align the samples on a surface profiler for the measurement [10]. For reference, the layout and the cross section of a partially etched test structure are displayed in Fig. 1 a). and b). The wafer with the test structures was diced into chips 11 mm long and 5 mm wide. Each chip contained 8 test structure arrays. The sacrificial layer was etched using varying process parameters for each chip. After the release, the bridge array was scanned by a surface profiler. During the measurement, the bridges where the sacrificial layer has been etched were deflected by the height of the sacrificial layer. If the target layer (SiO_2 or SiN) has also been removed, the total deflection of the bridge is the height of the sacrificial and the target layer. If the bridge has not been fully released, the extent of etching is still revealed by the deflection of the bridge. The etch undercut of the sacrificial layer is equal to half of the width of the widest bridge deflected by the height of the sacrificial layer. The etch undercut of the target layer is obtained similarly. It is half of the widest bridge deflected by the height of both the target and the sacrificial layer. An example of the resulting surface profile is presented in Fig. 1 c), it shows the signal that would result from the partially etched structure depicted in the cross-section of Fig. 1 b). The accuracy of this measurement was previously verified by imaging the cross sections of five randomly selected samples [10]. In all cases, the cross sectional images were in full agreement with the surface profile.

In total, five 100 mm diameter wafers were prepared with different layer configurations of materials available to the authors, diced into chips and used for this experiment. For reference, the layer compositions are detailed in table 1. For example, two samples were prepared for silicon dioxide measurements. The first was a reference sample, with a 500 nm thick layer of PECVD silicon dioxide and no sacrificial layer, denoted *SiO_2-Reference*. The second sample also has a 500 nm thick PECVD SiO_2 layer, this time covered by a 500 nm thick polysilicon sacrificial layer, denoted *SiO_2-PECVD*. A 50 nm thick platinum layer with a 10 nm thick titanium adhesion layer was used as an etch stop for both samples.

A 350 nm thick aluminium layer was sputter deposited on to all the samples. After photolithographic patterning of the layout displayed in Fig. 1 a), the aluminium and the polysilicon sacrificial layer were reactive ion etched (RIE). The exposed SiN and SiO_2 were also patterned using RIE in order to provide the vapour etch access to the layered stack to be etched. After resist removal, the wafers were cleaned in an oxygen plasma and diced.

III. Experiment

Before starting an experimental session, the vapour etch tool chamber was vented, and a standard etch process was run on an empty chamber. Then, another tool-specific calibration run was performed to determine the gas flows. After the temperature of the pedestal was adjusted to the desired value, the chamber was vented, and the sample loaded. At this point the etch recipe was programmed, and the etch process started. The tool enables control of the pressure, carrier gas flow and etch time with reactants flowing into the reaction chamber continuously.

TABLE II

THE EFFECT OF ADJUSTING THE ETCH PARAMETERS XeF_2 FLOW, PRESSURE AND TEMPERATURE ON THE ETCH RATE.

Sample ID	***Material***	***Flow XeF_2***[†] [µm min^{-1} $sccm^{-1}$]	***Pressure*** [µm min-^{1} $Torr^{-1}$]	***Temperature*** [µm min^{-1} K^{-1}]
SiN-PECVD	Polysilicon	- 0.31	2.24	- 0.14
	PECVD SiN	- 0.44	2.56	0.15
SiN-LPCVD	Polysilicon	- 0.2	1.8	-0.156
	Si_3N_4	Constant	-0.13	Constant
SiO_2-PECVD	Polysilicon	- 2.6	1.97	-0.128
	SiO_2	Constant	-0.19	Constant

[†]pressure constant at 9 Torr

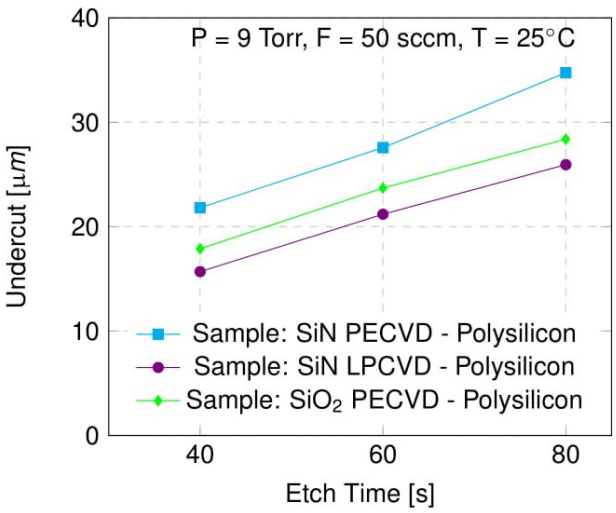

Fig.2 Polysilicon etch undercut over time

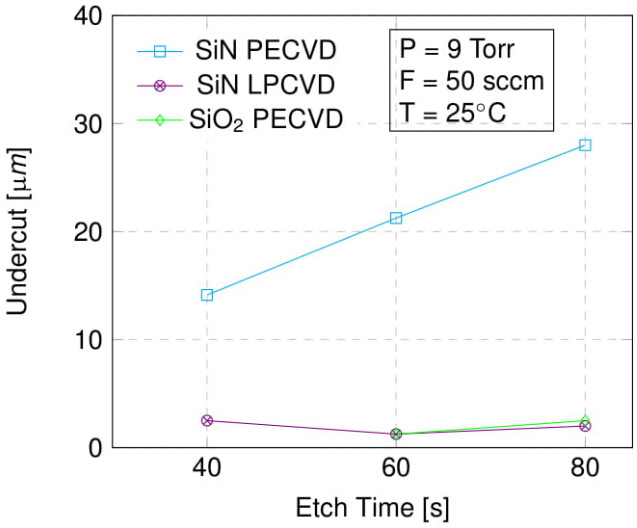

Fig. 3 The etch of the target materials as a function ot time

The chamber pressure and the carrier gas flow vary by less than 0.5 % during processing. The amount of XeF_2 carried into the chamber, however, depends on the amount of solid XeF_2 within the bubbler. It slowly decreases over the long term (10 – 20 of hours of etch time). It also decreases when running etch processes in rapid succession. It then recovers again after a break of roughly one hour. This must be taken into account when conducting more extensive experiments. The level of XeF_2 supplied to the chamber has a significant impact on the etch rate and is, therefore, the largest source of error. An external cooling and heating unit controls the pedestal temperature. When operating within the range of roughly 10 – 35 °C the temperature displayed on the external unit is equal to the measured temperature of the pedestal. For values outside this range, an additional measurement of the pedestal temperature was made for assurance. Undercut etching at the edges of the diced chips can be expected. While no silicon loading was observed in this experiment, it can occur if larger samples are processed, or if the XeF_2 concentration within the reaction chamber is lower. In that case, the loading effect can be reduced by covering the edges of the sample.

IV. Results

Three variable process parameters typically define the vapour etch process, the chamber pressure, the etch time and the XeF_2 gas flow into the chamber. In this experiment, two additional parameters are considered, the chamber temperature and the flow of additional gases, specifically hydrogen. The experiment was conducted on chips from the five samples described above. The *SiN-Reference* and *SiO_2-Reference* samples could not be measured using the test structure because the etch rates were below the limit of detection. This observation is critical, as these benchmark samples suggest very high selectivities of SiO_2 and SiN towards XeF_2. However, the SiO_2, PECVD SiN and LPCVD Si_3N_4 layers etched when placed in proximity to the sacrificial layer. The following section describes the results of this proximity etching in more detail, and the observations are summarized in Table II.

A. Impact of the etch parameters on the etch rates

Fig. 2 shows that the removal of sacrificial polysilicon is linear over time with etch rates between 392 nm/s and 545 nm/s being measured. The spread of the etch rates suggests that different etch by-products can affect the rate of polysilicon removal. It is possible that the proximity effect does not only affect the target material but also increases the etch rate of the sacrificial layer. From Fig. 3, it can be observed that the PECVD silicon nitride is etched at a rate of 347 nm/s, and follows the same linear trend.

In contrast, the undercuts for the LPCVD SiN and the PECVD SiO_2 appear to be independent of time. This can be explained by the etch halting once the fluorine radical generating materials in its proximity have been fully removed. The PECVD SiO_2 sample that was etched for 40 seconds could not be adequately measured and therefore, does not have a data point. Fig 4. presents three graphs, which show that the etch rate linearly decreases with increased XeF_2 flow. This seems counter-intuitive, but there are two possible explanations. Firstly, the XeF_2 is supplied through a bubbler, and the flow increase is achieved by increasing the carrier gas flow. The decline in the etch rate with increased XeF_2 flow, as displayed in Fig. 4, can be explained by the larger carrier gas flows required to supply the reactant. For instance, if 25 sccm of N_2 is used as the carrier gas, roughly 16 sccm XeF_2 are transported to the chamber. This corresponds to a ratio of around 3 to 2. However, if 100 sccm of N_2 was used as the carrier gas, roughly 36 sccm of XeF_2 flows into the chamber, corresponding to a ratio of around 3 to 1. This suggests that the XeF_2 partial pressure decreases with increasing carrier gas flow.

Secondly, the carrier gas flow determines the time it takes for the chamber to ramp up to the processing pressure, with lower

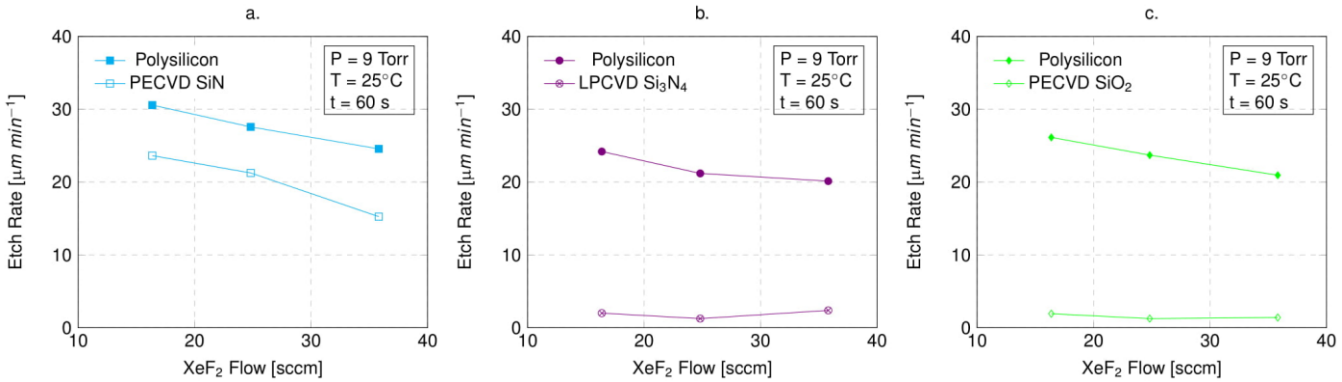

Fig. 4 The XeF_2 flow dependency of the etch rate at a pressure of 9 Torr, 25°C and an etch time of 60 seconds. a) polysilicon towards PECVD SiN b) Polysilicon towards LPCVD Si_3N_4 and c) polysilicon towards PECVD SiO_2.

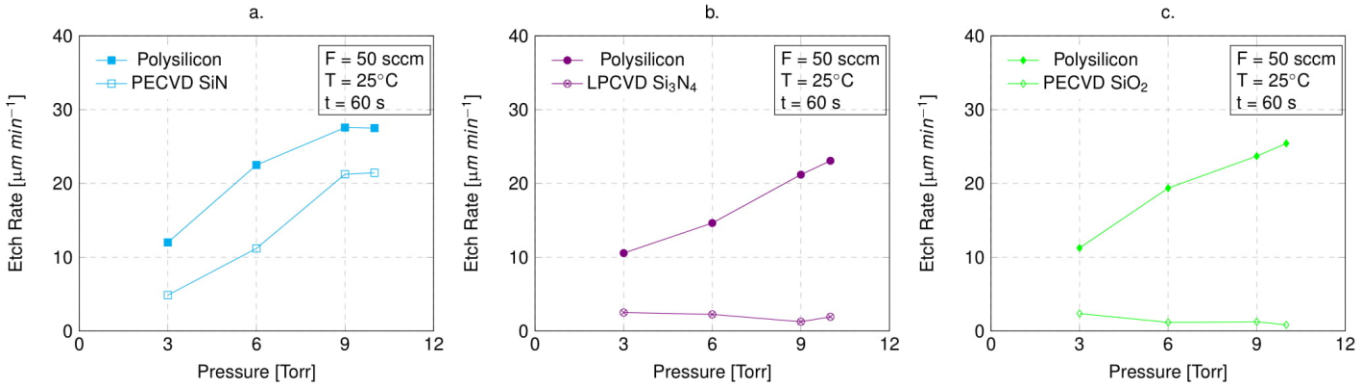

Fig. 5 The pressure dependency of the etch rate a) Polysilicon towards PECVD SiN b) Polysilicon towards LPCVD Si_3N_4 c) Polysilion towards PECVD SiO_2.

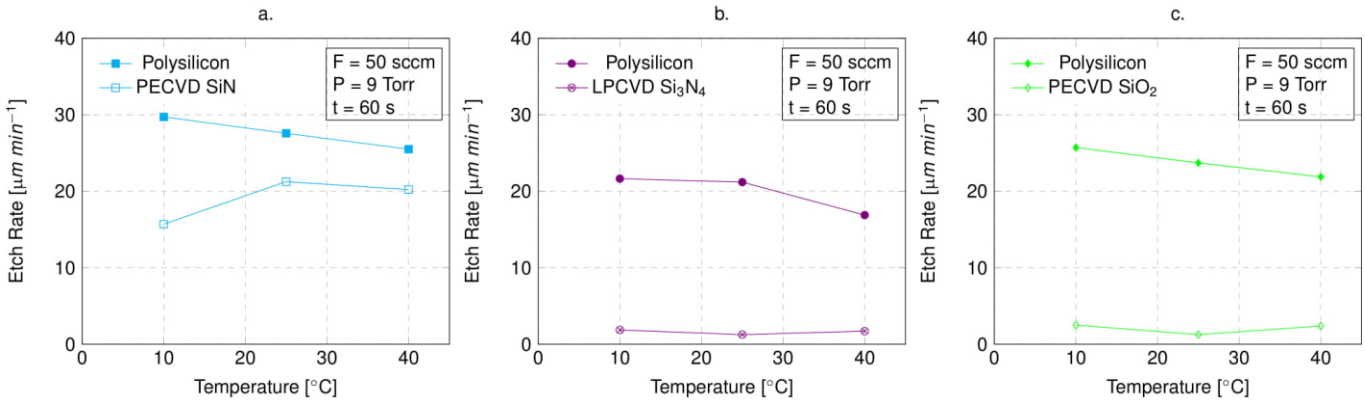

Fig. 6 The temperature dependency of the etch rate a) Polysilicon towards PECVD SiN b) Polysilicon towards LPCVD Si_3N_4 c) Polysilion towards PECVD SiO_2.

flows resulting in longer ramp times. With XeF_2 etchant being supplied to the chamber during the ramp time, the effective etch time increases with lower gas flows. As this is not taken into account when calculating the etch rate, the apparent etch rate appears to be higher. The tool's in-built etch monitor measures the amount of silicon fluorine bonds in the reaction chamber and gave a response of 1491, 1072 and 790 counts for XeF_2 gas flows of 16.4 sccm, 24.8 sccm and 35.8 sccm respectively. This indicates a higher level of SiF_4 within the reaction chamber at lower XeF_2 flows. The PECVD silicon nitride and polysilicon etch rates also appear to be similarly affected by the gas flows. However, the LPCVD silicon nitride and the PECVD silicon dioxide etch rates are not observed to correlate in the same way. The data presented in Fig. 5 show the effect that the processing pressure has on the removal of polysilicon and the respective target materials. The data indicates that there is a correlation between the processing pressure and etch rate. For polysilicon, it indicates, that increased processing pressure increases the etch rate. The same effect takes place with the PECVD silicon nitride. In contrast, the etch rate varies very little with increased pressure for the LPCVD silicon nitride and the PECVD silicon dioxide.

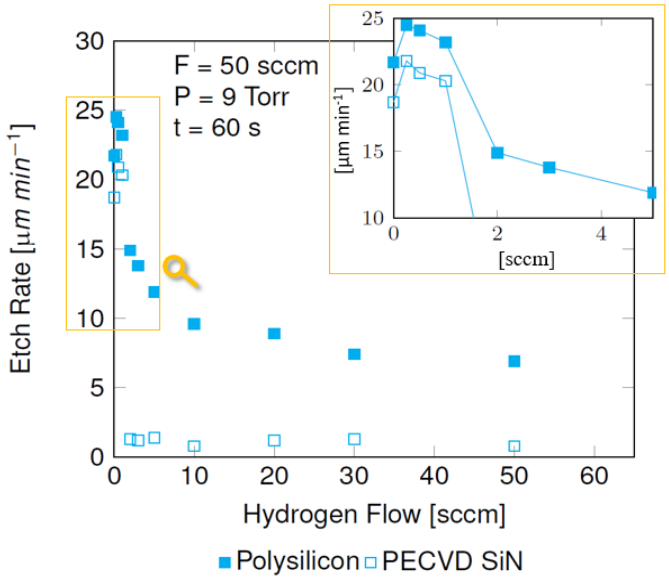

Fig. 7 Polysilicon and PECVD SiN etch rates of sample PECVD SiN relative to the amount of hydrogen supplied to the etch chamber.The inset magnifies the data for the hydrogen flows of 0 to 4 sccm

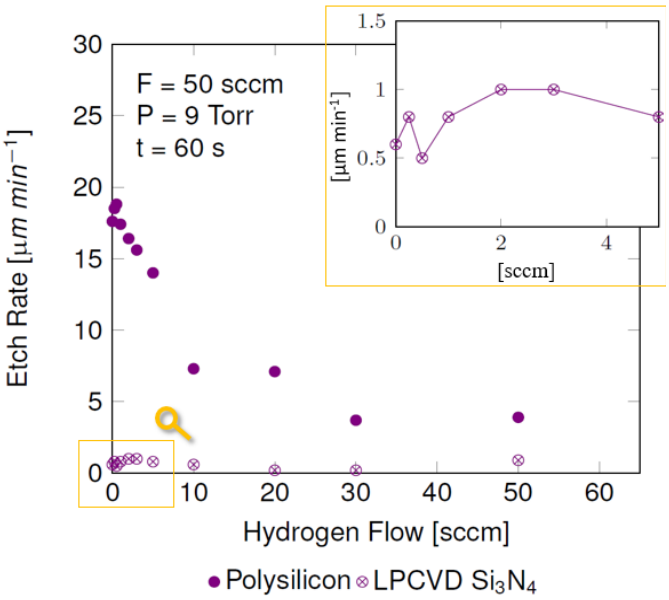

Fig. 8 Polysilicon and thermally grown Si3N4 of sample LPCVD SiN relative to the amount of silicon supplied to the chamber. The inset magnifies the data for the hydrogen flows of 0 to 4 sccm.

The data presented in Fig. 6 indicates a temperature dependency of the etch rate of the polysilicon and the target PECVD SiN. The polysilicon etch rate linearly decreases with increasing temperature at a rate between 128-159 nm/min/°C. This temperature-dependent etch rate decrease was expected, as it has been reported before by Chang et al. [5] and Ibbotson et al. [18] and is coherent with theories developed by Flamm et al. [15] and Vugts et al. [19]. In contrast, the PECVD silicon nitride etch rate increases with increasing temperature with a rate of roughly 150 nm/min/°C. The etch rate of the LPCVD silicon nitride, and the PECVD silicon dioxide appears to be unaffected by the change in temperature.

The data presented in Fig. 6 indicates a temperature dependency of the etch rate of the polysilicon and the target PECVD SiN. The polysilicon etch rate linearly decreases with increasing temperature at a rate between 128-159 nm/min/°C. This temperature-dependent etch rate decrease was expected, as it has been reported before by Chang et al. [5] and Ibbotson et al. [18] and is coherent with theories developed by Flamm et al. [15] and Vugts et al. [19]. In contrast, the PECVD silicon nitride etch rate increases with increasing temperature with a rate of roughly 150 nm/min/°C. The etch rate of the LPCVD silicon nitride, and the PECVD silicon dioxide appears to be unaffected by the change in temperature.

The addition of hydrogen has a significant effect on the etch rates of polysilicon and both PECVD and LPCVD silicon nitride. Both Fig. 7 and 8 show that the polysilicon etch rate increases by roughly 9% as the hydrogen flow is increased to 0.5 sccm. A further increase of the hydrogen flow leads to a sharp reduction of polysilicon etch rate. For example, the etch rate drops from 25 µm/min for a hydrogen flow of 0.5 sccm to 10 µm/min at a flow of 10 sccm. After this sharp decrease, the etch rate stabilizes and decreases slowly as the hydrogen flow is increased. For the *PECVD SiN*, the effect is even more pronounced. The etch rate sharply drops from 20 µm/min at a hydrogen flow of 1 sccm to 1 µm/min for a flow of 2 sccm. Beyond that point, additional hydrogen does not seem to reduce the etch rate any further. The general etch rates of the LPCVD silicon nitride are very low, which makes accurate measurements difficult. Fig. 8 shows a slight decrease in the etch rate from 1 µm/min without hydrogen to 0.2 µm/min with the addition of 30 sccm hydrogen. During this experiment, the XeF_2 flow fluctuated by roughly 1.3 sccm. Five samples were etched at a constant XeF_2 flow of 24.85 sccm. For these, a linear decrease of roughly 160 nm/min per sccm of hydrogen was observed between hydrogen flows of 0 and 20 sccm. At 30 sccm, no further decrease was observed.

A similar experiment was conducted for the *PECVD-SiO_2* samples. The hydrogen addition did not change the etch rate of the SiO_2. Four samples were etched for 300 seconds, with 0, 1, 3 and 10 sccm hydrogen additions. The silicon dioxide undercuts varied between 2.1 and 2.6 µm, indicating an etch rate of 0.42 to 0.52 µm/min. The standard deviation of the undercuts lay between 0.2 and 0.6 µm. Similarly, four more samples were etched for 120 seconds using the same conditions and hydrogen flows as for the previous samples. Again, the etch undercuts were between 2.3 and 2.6 µm and showed no correlation with the hydrogen flow into the chamber. The very similar undercuts measured on the samples etched for 120 seconds and 300 seconds indicate that the SiO_2 etch stops once the polysilicon in the proximity of it has been entirely removed.

B. Impact of the etch parameters on the selectivity

The selectivities that can be calculated from the data presented in figs 2 to 8, and the conditions under which they were obtained are summarized in table III.

While the PECVD silicon nitride selectivity does not appear to correlate with the XeF_2 flow, the selectivity of polysilicon towards silicon dioxide and the LPCVD silicon nitride does slightly increase at a flow rate of 25 sccm XeF_2. The change of the pressure does not have a significant impact on the selectivity in any of the presented material combinations. The temperature, however, does have an impact with the polysilicon etch rate decreasing with rising temperatures, while the etch rates of the LPCVD silicon nitride and the PECVD silicon dioxide remain constant. This causes a decrease in selectivity with increasing temperatures. This effect is even more pronounced for polysilicon and PECVD silicon nitride.

The addition of hydrogen has a significant impact on the polysilicon to PECVD silicon nitride selectivity. It rapidly improves from roughly 1.2:1 to 12.8:1 when the hydrogen flow is increased from 0 to 10 sccm. However, the 10 times increased selectivity is at the expense of decreasing polysilicon etch rate (from 22.4 to 9.6 µm/min). Increasing hydrogen additions leads to a decrease in selectivity because the polysilicon etch rate decreases faster than the silicon nitride etch rate beyond this threshold. The polysilicon to LPCVD silicon nitride selectivity also strongly improved with the addition of hydrogen. The maximum selectivity was measured at 38:1 for a 0.5 sccm hydrogen flow to the chamber. The lowest selectivity is reached at 10 sccm, with 12.3:1. The addition of hydrogen did not appear to have any impact on the SiO_2 etch rate. Unexpectedly, the polysilicon and PECVD silicon nitride etch rates are higher at 0.5 and 1 sccm hydrogen flows, than they are without any hydrogen addition. It should be noted that the XeF_2 partial pressure within the reaction chamber decreases as the amount of hydrogen supplied increases.

V. Discussion

A. Proximity Effect

The first hypothesis presented in this work was that fluorine radicals are formed during the etching of polysilicon that can attack other materials. Two observations have been made that provide supporting evidence. Firstly, no etch could be measured for the reference samples where no polysilicon is present. However, all three materials were etched at a measurable rate when placed in proximity of the sacrificial polysilicon. This suggests that LPCVD Si_3N_4 and SiO_2 are inert to XeF_2 but are etched by the reaction product (fluorine) that is formed during the etching of the polysilicon. Secondly, as can be observed in Fig. 2 and Fig. 3, the linear increase of the polysilicon and PECVD SiN undercut over time suggests that they reach a steady-state and etch at a constant rate. In contrast to that, the SiO_2 and LPCVD Si_3N_4 begin to etch but seem to stop etching, once 2 – 3 µm have been undercut.

Both phenomena can be explained by the results of extensive research into the XeF_2 etch mechanics conducted by Hefty et al. [12], [14]. They concluded that the XeF_2 abstracts[1] a fluorine atom at a dangling bond of the silicon. The remaining XeF molecule is scattered into the gas phase and can follow either of two reaction paths. It can abstract the second fluorine atom on another dangling bond or dissociate and scatter the Xe and fluorine atom. The fluorine radicals that are scattered onto the silicon break Si-Si lattice bonds and gradually fluorinate the polysilicon forming SiF, SiF_2 and SiF_3. Finally, all Si-Si bonds are broken, and SiF_4 desorbs into the gas phase. They also suggested that the backscattering of fluorine radicals onto the silicon surface explains why the Si etch rate with XeF_2 is an order of magnitude larger than the reaction rate with F_2. It is highly likely that these backscattered fluorine atoms can react with the silicon dioxide or silicon nitride. Relative energy calculations conducted by Veyan et al. [9] for the reaction of XeF_2 abstraction generated fluorine with SiO_2 suggest that it is energetically favourable, releasing 15.9 eV exothermally.

Furthermore, Loewenstein [16] investigated the temperature-dependent etch rates of SiO_2, LPCVD Si_3N_4 and polysilicon in remote plasma-generated fluorine. The SiO_2 used was LPCVD and is not directly comparable with the PECVD SiO_2 used in this study. However, the polysilicon and the LPCVD Si_3N_4 used are very similar to the layers described here. From the data, polysilicon to LPCVD Si_3N_4 selectivities of 7.1:1 and 11.4:1 can be calculated for 16°C and 30°C respectively. Van de Ven et al. [26] reported a-Si: Si_3N_4 selectivity of 8:1 when etching with fluorine [15]. Both reference values are in good agreement with the polysilicon to LPCVD Si_3N_4 selectivity range of 8.5:1 to 12:1 reported here. The PECVD SiN etched at a very high rate, and the selectivities in proximity etching are very low. Apparently, it has been observed, that "plasma nitride" (PECVD SiN) etches at a similar rate or even more rapidly than Si in CF_4/O_2 plasmas [26] [27][28][15]. Assuming that they refer to PECVD SiN and that fluorine is the reactive species in the CF_4/O_2 plasma etching process, their observations are in excellent agreement with those presented here.

In the case of the reference samples, no fluorine was generated as no sacrificial polysilicon was available for fluorine abstraction. Therefore the reactant to etch silicon nitride and silicon dioxide was not available.

Regarding the etch rate to pressure plots displayed in Fig. 5, these indicate, that the etch reaction of the LPCVD Si_3N_4, and the SiO_2 ceases once the polysilicon in proximity has been etched away. At low pressures, when the polysilicon is etched more slowly and remains in the vicinity of the LPCVD Si_3N_4 and SiO_2 for a longer time, the structures etch for longer, and the etch rate is higher. Most likely, this is caused by the dynamics of molecular movement. The fluorine radicals have a limited mean free path and disperse as they scatter away from their point of origin. A critical concentration of fluorine is required to sustain the etch reaction of LPCVD Si_3N_4 and SiO_2. The reaction will therefore stop once the sacrificial layer etch front has travelled

[1] Abstraction describes the removal of an atom by a radical.

beyond its proximity. For the LPCVD Si_3N_4 and SiO_2 datasets presented here, this distance appears to be 2-3 µm.

In conclusion, the discussion above suggests that fluorine radicals are formed and scattered during the reaction of XeF_2 with silicon. Hence, it is highly likely that the proximity effect affects all materials that are etched by fluorine.

B. Effect of Temperature on selectivity

Having established that the formation of fluorine radicals causes the proximity effect, this work considered methods to improve the selectivity. The temperature dependence of the etch rate of silicon using XeF_2 is the first promising mechanism that was investigated.

Considering the Arrhenius equation:

$$E.R. = \mathrm{A}\, e^{-\left(\frac{E_a}{RT}\right)} \quad (1)$$

One would expect that the etch rate (E.R.) increases when the temperature (T) rises because the gas constant (R) and the pre-exponential factor (A) are constants and the activation energy (E_a) is positive. This behaviour has been observed for the etching of polysilicon, SiO_2 and high-temperature chemical vapour deposited Si_3N_4 with fluorine [16]. In contrast, Vugts et al. [19] observed the highest XeF_2 etch rates of silicon at 150 K. As the temperatures increases, the reaction rate decreases, reaching a minimum reaction probability of roughly 20% at around 400 K. The reaction rates then rise again in the temperature range of 600 K to 900 K. Ibbotson et al. [18] observed that the reaction rate to temperature plot behaves linearly at temperatures below 360 K and calculated a reaction activation energy for this temperature spectrum of -13.4 kJ/mol (-3.2 kcal/mol).

The data in Fig. 6 shows the same trend over a limited temperature range. The calculated reaction energies are significantly lower at -3.75kJ/mol (-0.9 kcal/mol). It is unclear why the activation energy is negative in this case. Ibbotson suggested that the XeF_2 forms a bound surface layer prior to etching [18]. This hypothesis does not fully agree with the etch mechanism described by Hefty et al. [12], [13]. However, the Brunauer-Emmett-Teller (BET) theory [29] suggests that the rate of molecular adsorption increases with decreased temperature. Possibly, the abstraction of the fluorine on the silicon dangling bonds increases at lower temperatures. This would be consistent with previous research that found that the reaction layer grows at an accelerated rate between 200 K and 250 K [19].

TABLE III

THE XeF_2 VAPOUR ETCH SELECITIVITIES AND THE RESPECTIVE ETCH CONDITIONS THEY WERE OBSERVED

Material Combination	*Selectivity*	*Condition*[††]	*Source*
Si: PECVD SiN	5: 4	Proximity Effect	Fig. 2 & 3
Si: PECVD SiN	1.9: 1	Low T (10°C)	Fig. 6. a
Si: PECVD SiN	12: 1	2 sccm H_2 added	Fig. 7
Si: LPCVD Si_3N_4	6.3: 1 – 17: 1	Proximity Effect	Fig. 2 & 3
Si: LPCVD Si_3N_4	12: 1	Low T (10°C)	Fig. 6 b
Si: LPCVD Si_3N_4	38: 1	0.5 sccm H_2 added	Fig. 8
Si: PECVD SiO_2	11.4: 1 – 19: 1	Proximity Effect	Fig. 2 & 3
Si: PECVD SiO_2	10.3: 1	Low T (10°C)	Fig. 2 & 3

[††]T: Temperature

Fig. 6 a. suggests that the etch rate of PECVD silicon nitride increases with increasing temperature. From the graph, the activation energy was calculated to be 6.221 kJ/mol (1.48 kcal/mol). Unfortunately, no reference value for the PECVD SiN fluorine etch activation energy could be obtained from the literature, but the value presented here appears reasonable. The data does not show a temperature correlation for the LPCVD Si_3N_4 and the SiO_2 samples. However, this does not mean that this is not the case, because the SiO_2 and LPCVD Si_3N_4 etch reaction could have stopped once the sacrificial layer had etched beyond the proximity etch distance as discussed earlier. The literature suggests that the SiO_2 and LPCVD Si_3N_4 reaction rates with fluorine are temperature dependent. Loewenstein [16] reported activation energies of 14.853 kJ/mol (3.55 kcal/mol) and 14.058 kJ/mol (3.36 kcal/mol) for LPCVD Si_3N_4 and SiO_2 respectively. Both reaction energies are positive. This implies an increased etch rate with increased temperature.

In summary, the data presented in this study and the literature suggests, that the selectivity of Si towards PECVD SiN, SiO_2 and LPCVD Si_3N_4 increases with decreasing temperature. However, the measurements also suggest, that significant selectivity improvements can only be expected at temperatures substantially below 0 °C. There are no vapour etch tools currently on the market that can operate in such a low-temperature regime.

C. Effect of hydrogen on selectivity

When hydrogen was added into the etch chamber it was, observed to have an impact on the etch selectivities of PECVD and LPCVD Si_3N_4. In particular, the PECVD SiN etch rate drops significantly. Assuming, that the fluorine radicals are causing the proximity etching effect it is reasonable to add hydrogen in order to form unreactive hydrogen fluoride HF according to;

$$H_2 + F \rightarrow HF + H \quad (2)$$

The hypothesis that the addition of hydrogen significantly reduces the number of reactive fluorine radicals, is supported by the decreasing polysilicon etch rates observed with increased hydrogen flows. However, the reaction is not completely halted for any of the materials investigated in this study. The reasons for this are unclear, and a detailed investigation is beyond the scope of this article. However, there are two possible explanations. Firstly, the formation of highly reactive hydrogen radicals as a product of the reaction in equation (2), might cause the continuous etching of these materials. A study into hydrogen plasma etching by Chang et al. [30] reported hydrogen radical etch rates of 15 Å/min for SiO_2 and LPCVD Si_3N_4 and 250 – 500 Å/min for silicon. These etch rates are roughly 10% of those reported here. However, the data is difficult to compare as it is unclear at which pressure their etch

rate data was obtained. An alternative mechanism might be the formation of hydrogen fluoride in an excited state, as presented by Volynet et al. [21] and Jung et al. [22]. They found that the presence of excited hydrogen fluoride brings additional energy to the reaction site, enabling a selective etch reaction of LPCVD Si_3N_4 over SiO_2. Interestingly, even though different materials were etched, both their work and this study observed maximum etch rates after the addition of hydrogen.

In summary, the addition of hydrogen significantly improves the etch selectivity of LPCVD Si_3N_4 and PECVD SiN towards polysilicon. However, the data related to the impact of hydrogen on the selectivity of SiO_2 towards polysilicon showed no enhancement. This may be due to the fluorine radicals and hydrogen forming unreactive HF. However, the detailed mechanisms involved are yet unclear, and further investigations are required to understand the chemistry fully.

VI. Conclusion

In conclusion, this paper provides strong evidence supporting the hypothesis that the selectivity of various fluorine reactive materials to polysilicon reduces significantly if they are exposed to the etch reactions by-products in close proximity (< 3 μm) to the sacrificial material during XeF_2 vapour etching. It is proposed that the fluorine radicals that form during the silicon etch, attack the LPCVD Si_3N_4, SiO_2, and PECVD SiN investigated in this study. For test structures used in this study, this resulted in selectivities as low as 6.3:1, 11.4 and 5:4 respectively. It should be remembered that these selectivities relate to the specific layout ("worst-case") and architecture of test structures employed in this work. Their value is that any process enhancements that improve their selectivity can be confidently adopted for structures more typical of MEMS devices. With the proximity effect inhibiting the design and manufacturing possibilities of MEMS and NEMS two methods to improve the selectivity have been identified:

(1) Reducing the process temperature by 15 ºC improved the PECVD SiN selectivity from 5:4 to 7.4:4. However, significant improvements can only be expected when operating at low subzero degrees Celsius temperatures. Current commercial tools that operate in this temperature regime are not available, but should it be required, enhanced cooling systems offer the opportunity to realize this potential for selectivity improvement in the future.

(2) Supplying hydrogen into the reaction chamber during etching yielded significant selectivity improvements. It is proposed that this improvement results from the fluorine radicals and the H_2 forming unreactive hydrogen fluoride molecules. This significantly reduces the etch rates of LPCVD Si_3N_4 and PECVD SiN. With the test structures at room temperature, the addition of hydrogen resulted in maximum selectivities of 38:1 and 12:1 for LPCVD Si_3N_4 and PECVD SiN respectively. A further advantage of hydrogen additions is that high polysilicon etch rates were maintained when using the hydrogen additions.

Clearly adding hydrogen to the XeF_2 vapour etch processes mitigates the proximity effect, and thereby creates new design and fabrication possibilities for MEMS and NEMS devices.

Acknowledgement

M.R thanks Norbert Radacsi, for his support while conducting this study. Furthermore, the authors thank memsstar Ltd for their helpful suggestions during the experimental design and results interpretation. The raw data underlying the finds reported in this work is available online from https://doi.org/10.7488/ds/2929 .

References

[1] J. R. Holt, R. C. Hefty, M. R. Tate, and S. T. Ceyer, "Comparison of the interactions of XeF2 and F2 with Si(100)(2 × 1)," *J. Phys. Chem. B*, vol. 106, no. 33, pp. 8399–8406, 2002.

[2] R. Maboudian and R. T. Howe, "Critical Review: Adhesion in surface micromechanical structures," *J. Vac. Sci. Technol. B Microelectron. Nanom. Struct.*, vol. 15, no. 1, p. 1, 1997.

[3] U. Zaghloul, G. Papaioannou, B. Bhushan, F. Coccetti, P. Pons, and R. Plana, "On the reliability of electrostatic NEMS/MEMS devices: Review of present knowledge on the dielectric charging and stiction failure mechanisms and novel characterization methodologies," *Microelectron. Reliab.*, vol. 51, no. 9–11, pp. 1810–1818, 2011.

[4] H. F. Winters and J. W. Coburn, "The etching of silicon with XeF2 vapor," *Appl. Phys. Lett.*, vol. 34, no. 1, pp. 70–73, 1979.

[5] F. I. Chang *et al.*, "Gas-phase silicon micromachining with xenon difluoride," *Microelectron. Struct. Microelectromechanical Devices Opt. Process. Multimed. Appl.*, vol. 2641, p. 117, 1995.

[6] V. M. Donnelly, "Review Article: Reactions of fluorine atoms with silicon, revisited, again," *J. Vac. Sci. Technol. A Vacuum, Surfaces, Film.*, vol. 35, no. 5, p. 05C202, 2017.

[7] H. F. Winters and D. Haarer, "Influence of doping on the etching of Si(111)," *Phys. Rev. B*, vol. 36, no. 12, pp. 6613–6623, 1987.

[8] P. B. Chu *et al.*, "Controlled Pulse-Etching with Xenon Difluoride."

[9] J. F. Veyan, M. D. Halls, S. Rangan, D. Aureau, X. M. Yan, and Y. J. Chabal, "XeF2-induced removal of SiO2near Si surfaces at 300 K: An unexpected proximity effect.," *J. Appl. Phys.*, vol. 108, no. 11, 2010.

[10] M. Rondé, A. J. Walton, and J. G. Terry, "Test Structure for Measuring the Selectivity in Vapour Etch Processes," in *IEEE 33rd International Conference on Microelectronic Test Structures (ICMTS), Edinurgh, United Kingdom*, 2020, pp. 1–5.

[11] M. Gorisse *et al.*, "Lateral Field Excitation of membrane-based Aluminum Nitride resonators," *Proc.*

IEEE Int. Freq. Control Symp. Expo., 2011.

[12] R. C. Hefty, J. R. Holt, M. R. Tate, and S. T. Ceyer, "Atom abstraction and gas phase dissociation in the interaction of XeF 2 with Si(100)," *J. Chem. Phys.*, vol. 129, no. 21, 2008.

[13] R. C. Hefty, J. R. Holt, M. R. Tate, D. B. Gosalvez, M. F. Bertino, and S. T. Ceyer, "Dissociation of a product of a surface reaction in the gas phase: XeF 2 reaction with Si," *Phys. Rev. Lett.*, vol. 92, no. 18, pp. 18–21, 2004.

[14] R. C. Hefty, J. R. Holt, M. R. Tate, and S. T. Ceyer, "Mechanism and dynamics of the reaction of XeF2 with fluorinated Si(100): Possible role of gas phase dissociation of a surface reaction product in plasmaless etching," *J. Chem. Phys.*, vol. 130, no. 16, 2009.

[15] D. L. Flamm and V. M. Donnelly, "The design of plasma etchants," *Plasma Chem. Plasma Process.*, vol. 1, no. 4, pp. 317–363, 1981.

[16] L. M. Loewenstein, "Temperature dependence of silicon nitride etching by atomic fluorine," *J. Appl. Phys.*, vol. 65, no. 1, pp. 386–387, 1989.

[17] D. E. Ibbotson, J. A. Mucha, D. L. Flamm, and J. M. Cook, "Plasmaless dry etching of silicon with fluorine-containing compounds," *J. Appl. Phys.*, vol. 56, no. 10, pp. 2939–2942, 1984.

[18] D. E. Ibbotson, D. L. Flamm, J. A. Mucha, and V. M. Donnelly, "Comparison of XeF2and F-atom reactions with Si and SiO2," *Appl. Phys. Lett.*, vol. 44, no. 12, pp. 1129–1131, 1984.

[19] M. J. M. Vugts, G. L. J. Verschueren, M. F. A. Eurlings, L. J. F. Hermans, and H. C. W. Beijerinck, " Si/XeF 2 etching: Temperature dependence ," *J. Vac. Sci. Technol. A Vacuum, Surfaces, Film.*, vol. 14, no. 5, pp. 2766–2774, 1996.

[20] B. E. E. Kastenmeier, P. J. Matsuo, and G. S. Oehrlein, "Highly selective etching of silicon nitride over silicon and silicon dioxide," *J. Vac. Sci. Technol. A Vacuum, Surfaces, Film.*, vol. 17, no. 6, pp. 3179–3184, 1999.

[21] S. Rachidi *et al.*, " Isotropic dry etching of Si selectively to Si 0.7 Ge 0.3 for CMOS sub-10 nm applications ," *J. Vac. Sci. Technol. A*, vol. 38, no. 3, p. 033002, 2020.

[22] V. Volynets *et al.*, " Highly selective Si 3 N 4 /SiO 2 etching using an NF 3 /N 2 /O 2 /H 2 remote plasma. I. Plasma source and critical fluxes ," *J. Vac. Sci. Technol. A*, vol. 38, no. 2, p. 023007, 2020.

[23] J.-E. Jung *et al.*, " Highly selective Si 3 N 4 /SiO 2 etching using an NF 3 /N 2 /O 2 /H 2 remote plasma. II. Surface reaction mechanism ," *J. Vac. Sci. Technol. A*, vol. 38, no. 2, p. 023008, 2020.

[24] K. Sugano and O. Tabata, "Etching Rate control of mask material for XeF2 etching using uv exposure," *Micromach. Microfabr. Process Technol. VII*, vol. 4557, no. September 2001, pp. 18–23, 2001.

[25] U. Streller, A. Krabbe, and N. Schwentner, "Selectivity in dry etching of si(100) with XeF 2 and VUV light," *Appl. Surf. Sci.*, vol. 106, pp. 341–346, 1996.

[26] E. Van de Ven, T. . Shankoff, and R. Heinecke, "Gas etching of dielectrics and metals," Harlow, Essex, 1973.

[27] R. L. Maddox, "Applications of reactive plasma practical microelectronic processing systems," *Solid State Technol.*, vol. 21, no. 4, p. 107, 1978.

[28] A. Jacob, "The Versatile Technique of RF Plasma Etching. III. Mechanistic Considerations for Selective Etching," *Solid State Technol.*, vol. 21, no. 4, pp. 95–98, 1978.

[29] B. S. Brunauer and P. H. Emmett, "Adsorption of Gases in Multimolecular Layers," no. lc, 1938.

[30] R. P. H. Chang, C. C. Chang, and S. Darack, "Hydrogen Plasma Etching of Semiconductors and Their Oxides.," *J. Vac. Sci. Technol.*, vol. 20, no. 1, pp. 45–50, 1982.